Regime shifts, alternative states and hysteresis in the *Sarracenia* microecosystem

Matthew K. Lau[1], Benjamin Baiser[2], Nicholas J. Gotelli[3] and Aaron M. Ellison[1*]

1. Harvard Forest, Harvard University, 324 North Main Street, Petersham, Massachusetts 01366; 2. Department of Wildlife Ecology and Conservation, University of Florida, Gainesville, Florida 32611; 3. Department of Biology, University of Vermont, Burlington, Vermont 05405. * Corresponding author; e-mail: aellison@fas.harvard.edu

Manuscript elements: TBD.

Keywords: alternative states, model system, organic-matter loading, regime shifts, *Sarracenia purpurea*

Manuscript type: Article.

Abstract

Changes in environmental conditions can lead to a rapid shift in the state of an ecosystem ("regime shift"), which subsequently returns to the previous state slowly, if ever ("hysteresis"). Studies of ecological regime shifts have been hampered by the large spatial and temporal scales over which they occur and the lack of a common framework linking observational and experimental data to models. The naturally-occurring aquatic micro-ecosystem inside leaves of the northern pitcher plant (*Sarracenia purpurea*) occurs in both oligotrophic and eutrophic states. These alternative states also can be induced experimentally by enriching oligotrophic pitchers with additional insect prey, which elevates oxygen demand by microbes and leads to rapid eutrophication. This regime shift of the *Sarracenia* micro-ecosystem has been modeled with discrete-time difference equations that include parameters for the photosynthetic rate of the pitcher plant, consequent diffusion of oxygen through the pitcher liquid, rate of prey input, and biological oxygen demand by microbes as they decompose and mineralize the prey. We elaborated the regime-shift model of the *Sarracenia* micro-ecosystem and used sensitivity analysis to identify the parameters that control most strongly the dynamics of the system as it switches between oligotrophic and eutrophic states. Three main findings emerged. 1) Simulations accurately captured the regime shift and subsequent hysteresis that follows from prey enrichment; 2) When modeled as a modified Hill function, the interaction of prey input and decomposition rates drove the regime shift; 3) The interaction between biological oxygen demand of the food web and decomposition rate yielded a threshold that altered the hysteresis dynamics, shifting the sign of the effect of increasing the oxygen demand parameter. Because the model of the *Sarracenia* micro-ecosystem displays behaviors that are qualitatively similar to larger scale models of dynamic systems, we suggest that the *Sarracenia* micro-ecosystem itself represents a valuable and scalable experimental system for studying ecological regime shifts.

Introduction

Regime shifts in ecological systems are defined as rapid changes in the spatial or temporal dynamics of a more-or-less stable system caused by slow, directional changes in one or more underlying state variables (e.g., Scheffer et al. 2009, 2001). In the last several years, many researchers have suggested that a wide range of ecological systems are poised to "tip" into new regimes (Petraitis and Dudgeon 2016; Scheffer et al. 2009), or even that we are approaching a planetary tipping point (Barnosky et al. 2012; but see Brook et al. 2013). Because changes in the underlying state variables of most ecosystems occur over time spans of years to centuries, our understanding of the causes and consequences of ecological regime shifts has progressed slowly. More rapid progress can be achieved by working with well-understood model systems that can be described mathematically and manipulated experimentally over short time scales.

It is rare to find an ecological systems in which the occurrence of a regime shift and its cause-and-effect relationship with one or more underlying environmental drivers is unambiguous (Bestelmeyer et al. 2011). This is primarily because long time series of observations collected at meaningfully large spatial scales are required to identify the environmental driver(s), its relationship to the response variable of interest, the stability of each state, the breakpoint between them, and hysteresis in the return time to the original state (Bestelmeyer et al. 2011; Petraitis and Dudgeon 2016). Detailed modeling and decades of observations and experiments have led to a thorough understanding of one canonical example of an ecological regime shift: the rapid shift from oligotrophic to eutrophic states in lakes (e.g., Carpenter and Brock 2006; Carpenter et al. 2011). The primary difficulties with using lakes as models for studying alternative states and ecological regime shifts are their large size (which precludes extensive replication: Carpenter 1998) and the long time scales (decades) required to observe a regime shift, subsequent ecosystem hysteresis, and eventual recovery (Contamin and Ellison 2009; Mittlebach et al. 1995). Models of lake ecosystems and their food webs, and associated empirical data, have revealed that returning lakes from a eutrophic to an oligotrophic state can be very slow—on the order of decades to cen-

turies—(Contamin and Ellison 2009) and depends not only on slowing or reversing directional changes in underlying state variables but also on the internal feedback dynamics of the system. Other aquatic systems, including fisheries (Biggs et al. 2009) and intertidal zones and reefs (Petraitis and Dudgeon 2016), have provided additional empirical support for these model results, both in dynamics and duration (Dakos et al. 2012).

Recently, we have shown experimentally that organic-matter loading (i.e., prey addition) can cause a shift from oligotrophic to eutrophic conditions in a naturally-occurring micro-ecosystem: the water-filled leaves of the northern (or purple) pitcher plant, *Sarracenia purpurea* L. (Sirota et al. 2013). Because bacteria that reproduce rapidly drive the nutrient-cycling dynamics of the five-trophic level *Sarracenia* micro-ecosystem (Butler et al. 2008), the system shifts from oligotrophic to eutrophic states in hours or days rather than years or decades. Further, the comparatively small volume of individual pitchers, the ease of growing them in greenhouses, and the occurrence of large, experimentally manipulable populations in the field has allowed for replicated studies of trophic dynamics and regime shifts in a whole ecosystem (Srivastava et al. 2004). Here, we extend Sirota et al.'s (2013) mathematical model of the *Sarracenia* micro-ecosystem, introduce more realism into the underlying environmental drivers of the model and use sensitivity analysis to identify the parameters that most strongly control the dynamics of the system. Through this examination of its dynamics, we show that this micro-system eventually can overcome its hysteresis and return to an oligotrophic state once organic-matter input is stopped. The model is sufficiently general and illustrates dynamic behaviors that are qualitatively similar to models of regime shifts in lakes and other ecosystems. We suggest, therefore, that the *Sarracenia* micro-ecosystem is a scalable model for studying ecological regime shifts in real time.

Methods

The Pitcher Plant Micro-ecosystem

Pitcher plants (*Sarracenia* spp.) are perennial carnivorous plants that grow in bogs, poor fens, seepage swamps, and sandy out-wash plains in eastern North America (Schnell 2002). Their leaves are modified into tubular structures, or "pitchers", (Arber 1941) that attract and capture arthropods and occasionally small vertebrate prey (e.g., Butler et al. 2005; Ellison and Gotelli 2009). In the pitchers, prey are shredded by obligate pitcher-inhabiting arthropods (including Histiostomatid *Sarraceniopus* mites, and larvae of Sarcophagid (*Fletcherimyia fletcheri*) and Chironomid flies (*Metrocnemius knabi*) (Addicott 1974; Heard 1994; Jones 1923). The shredded organic matter is further decomposed and mineralized by a diverse assemblage of microbes, including protozoa (Cochran-Stafira and von Ende 1998), yeasts (Boynton 2012), and bacteria (Peterson et al. 2008).

Unlike other species of *Sarracenia* that also secrete and use digestive enzymes to extract nutrients from their captured prey, *S. purpurea* secretes digestive enzymes at most for only a few days (Gallie and Chang 1997). In the main, *S. purpurea* relies on its aquatic food web to decompose the prey and mineralize their nutrients (Butler and Ellison 2007). As a result, the rainwater-filled pitchers of *S. purpurea* are best considered a detritus (prey)-based ecosystem in which bacterially-mediated nutrient cycling determines whether it is in an oligotrophic or eutrophic state (Bradshaw and Creelman 1984; Butler et al. 2008; Sirota et al. 2013).

Although the dynamics of the *Sarracenia* micro-ecosystem are very similar to those of lakes and streams, there is one important difference. Lake food webs are "green" (plant-based), while pitcher plant food webs are "brown" (detritus-based) (Butler et al. 2008). In lakes, the shift to a eutrophic state occurs through addition of limiting nutrients (usually N or P), accumulation of producer biomass that is uncontrolled by herbivores (see Wood et al. 2016), and subsequent decomposition that increases biological oxygen demand (Carpenter et al. 1995; Chislock et al. 2013). The *Sarracenia* micro-ecosystem's "brown" food web also experiences an increase in oxygen

demand and microbial activity; however, this occurs during the breakdown of detritus that is characteristic of its shift from an oligotrophic to a eutrophic state (Sirota et al. 2013).

Oxygen dynamics in lakes and pitchers

Oxygen dynamics in both lakes and Sarracenia pitchers can be described using a simple model that yields alternative oligotrophic and eutrophic states and hysteresis in the shift between them (Scheffer et al. 2001):

$$\frac{dx}{dt} = a - bx + rf(x) \tag{1}$$

In Scheffer's model, the observed variable x (e.g., oxygen concentration) is positively correlated with state variable a (e.g., rate of nutrient input or photosynthesis) and negatively correlated with state variable b (e.g., rate of nutrient removal or respiration). The function $rf(x)$ defines a positive feedback that increases x (e.g., the rate of nutrient recycling between the sediment in lakes or mineralization-immobilization by bacteria of shredded prey in a water-filled *Sarracenia* pitcher). If $r > 0$ and the maximum of $\{rf(x)\} > b$, there will be more than one equilibrium point (i.e., stable state) (Scheffer et al. 2001); the function $f(x)$ determines the shape of the switch between the states and the degree of hysteresis. Following Scheffer et al. (2001), we use a Hill function for $f(x)$:

$$f(x) = \frac{x^p}{x^p + h^p} \tag{2}$$

The Hill function provides a simple model that can produce threshold behavior. The inflection point is determined by the parameter h (Fig. 1A). Given that the other parameters are set so that there are alternative states (i.e. $rf(x) > b$), h determines the threshold for the transition between the alternative states. When viewed in a phase-space (Fig. 1B), the transition between states can be seen as a path traversed by the system between distinct regions (i.e. phases). In part because of this threshold property, the Hill function has been applied to systems in

biochemistry, microbiology and ecology whose dynamics depend on a limiting resource (see Mulder and Hendriks 2014).

We model the dynamics of the trophic state of the *Sarracenia* micro-ecosystem using an equation of the same underlying form as 1:

$$x_{t+1} = \underbrace{a_t A_t}_{\text{Photosynthesis}} - \underbrace{\left\{ m + a_t \left[\frac{w_{t-1}}{w_{t-1} + K_w} \right] \right\}}_{BOD} + \underbrace{D_t(x_t)}_{Diffusion} \tag{3}$$

$$a_{t+1} = a_t \times \left\{ \frac{a'_{max} - a'_{min}}{1 + e^{-s \cdot n_t - d}} + a'_{min} \right\} \tag{4}$$

Each model term is described below and summarized in Table 1.

The model (Eq. 3) of the *Sarracenia* micro-ecosystem (Fig. 2A) is made up of the two main terms: production of oxygen by photosynthesis and use of oxygen (respiration) during decomposition (BOD: biological oxygen demand). The pitcher fluid is oxygenated (x) at each discrete time step (t) as the plant photosynthesizes (A_t). The value of A_t is determined by sunlight, which we model as a truncated sine function producing photosynthetically active radiation (PAR) (Fig. 2B), and by the maximum photosynthetic rate (A_{max}), (Fig. 2C), which leads to the production of dissolved oxygen in the pitcher fluid (Fig. 2D).

Decomposition of shredded prey by bacteria requires oxygen. The oxygen demand from respiration is modeled by the BOD term in Eq. 3. The parameter m is the basal metabolic respiration of the food-web with no prey to decompose in the system. Adding prey (w) induces decomposition, which we model as a negative exponential function with rate parameter β and a constant W (maximum prey mass decomposed over 48 hours), per Eq. 5, which is shown in Figure 2E. Bacterial populations increase at a rate determined by a half-saturation function with parameter K_w (Eq. 3), which increases BOD and the depletion of oxygen from the pitcher fluid (Fig. 2F).

$$w_{t+1} = w_t \cdot e^{-\beta \cdot W} \tag{5}$$

Thus, the food-web demand for oxygen (i.e. BOD) depends on the decomposition rate (β) and

the shape parameter (K_w), but only when prey is present in the system ($w_{t-1} > 0$ in Eq. 3). When prey is absent (i.e. $w_{t-1} = 0$), BOD terms simplifies by multiplication to the basal metabolic rate (m).

The other impact of prey addition and subsequent decomposition by the food-web is the release of nutrients into the pitcher fluid. The mineralization variable n_t (Eq. 3), which is modeled as proportionate to the product of the amount of oxygen and prey in the system (i.e. $n_{t+1} = c \cdot (w_t \cdot x_t)$, where c is a constant of proportionality), creates a feedback from decomposition to oxygen production by the plant (i.e. the path in Fig. 2A from the food-web to nutrients to pitcher to oxygen and back to the food-web). Photosynthesis is limited by available nutrients (primarily nitrogen and phosphorus, see Ellison 2006; Givnish et al. 1984) that are mineralized by bacteria from the prey (Butler et al. 2008). Photosynthesis is augmented (a_t) by nutrient mineralization rate (s). We model a_t as a saturating function with bounds determined by the range terms (a_{min} and a_{max}), s, and the point of saturation (d). Thus, the mineralization term couples respiration (oxygen depletion) to photosynthesis (oxygen production) when prey is introduced to the system and the food-web begins to decompose the prey and release nutrients into the pitcher fluid. Finally, a small amount of oxygen diffuses into the pitcher fluid directly from the atmosphere ($D(x)$), which is unlikely to influence the fluid oxygen at a rate that is negligible in comparison to photosynthesis or BOD.

Sensitivity Analysis

We used sensitivity analysis, in which we covaried the prey addition rate (w), decomposition rate (β), and the half-saturation constant K_w, to explore the behavior of the micro-ecosystem model. Rather than set combinations of fixed values for the three parameters of interest, We sampled the model parameter space using uniform distributions for each of them: $K_w \sim$ U(0.001, 1), $\beta \sim$ U(2.0E-6, 2.0E-5) and $w \sim$ U(0, 75). In addition, for each combination of β and K_w, one simulation was run without prey added to the system (w = 0) to characterize baseline (oligotrophic) oxygen concentrations. All simulations (n = 15000) started with an initial value for oxygen (x_0) and all

other variables set equal to 0, prey additions occurred at mid-day on days 4-6 (i.e. $t = 6480$ to $t = 9360$) and each ran for 30 simulation days (43,200 minutes); output was saved for each simulated minute. Although the simulations were initialized using a random sample of parameter values and run in parallel, the model is completely deterministic and, thus, the resulting runs can be reproduced by starting the simulations with the exact values used to initialize and parameterize the models, which are available via the Harvard Forest Data Archive (URL and DOI).

To aid in the detection of the impact of the most important parameters and variables, in all simulations we set some parameter values to zero, which altered the model in following two ways. First, we ignored the $D(x_t)$ term because we assumed that amount of oxygen diffusing directly into the pitcher fluid from the atmosphere would be orders of magnitude lower than oxygen produced by pitcher photosynthesis (Kingsolver 1979). Second, we noted that, since the basal metabolic respiration of the food-web parameter (m) is an additive constant, any change in the value of the constant m, (basal respiration of the microbial community) resulted only in a proportional change in value of x, not in the shape of the oxygen production over time. Therefore, we set $m = 0$ and in doing so were able to make an additional observation based on the form of the final equation that photosynthetic augmentation (a_t) influenced photosynthesis (A_t) and BOD ($\frac{w_{t-1}}{w_{t-1}+K_w}$) identically. Therefore, the parameters s and d in Eq. 4 could be ignored in the sensitivity analysis (i.e. not varied). These simplifications reduced the dimensionality of the analysis to three (w, β and K_w), greatly reducing the number of simulations and the complexity of the subsequent analyses.

We used the time series of x_t to calculate two measures of the state of the system: percent time anoxic and system return rate. We defined anoxia in the model to be an oxygen concentration of $\leq 0.05\ \mu\text{gL}^{-1}$. We measured the percent time the model spent in an "anoxic" state as the amount of time out of the total simulation time that the system spent below an oxygen value of 0.05 (see Sirota et al. 2013). We defined the return rate as the difference in oxygen concentration from the point at which prey was first added to the system to either the first point in time when the oxygen returned to the baseline oxygen level (i.e., without prey, in the oligotrophic state) or the

last maximum oxygen level prior to the end of the simulation over time, if the oxygen levels did not return to baseline. Return time was determined to a precision of 1.0E-5.

Based on the form of the terms used to model BOD, the BOD term should decrease exponentially when the parameters K_w and β, respectively, are increased. β controls the rate of decomposition and K_w controls the efficiency of prey decomposition by the microbial community. If β is increased and all other parameters are held constant, BOD will reach its maximum level more quickly. If K_w is increased and all other parameters are held constant, the efficiency of microbial decomposition should decrease BOD.

Code Availability and Execution

The model was coded in the **R** programming language (R Core Team 2016). The 15,000 model runs for the sensitivity analysis were run on the Odyssey Supercomputer Cluster at Harvard University (Research Computing Group, FAS Division of Science, Cambridge, Massachusetts). Data are available in the Harvard Forest Data Archive (http://harvardforest.fas.harvard.edu/harvard-forest-data-archive). Code for the simulations and subsequent analyses can be found at the Harvard Forest Github organization website: https://github.com/HarvardForest/SarrSens.

Results and Discussion

General theoretical work in complex systems has suggested that the definition of system boundaries is arbitrary and carries the potential for systems dynamics to be mechanistically connected but unpredictable from lower, more reduced scales of organization (Levine et al. 2016; Ulanowicz 2012). However, others have argued that food-web dynamics of whole ecosystems can be inferred from the components (i.e., motifs and modules) of these ecosystems (McCann 2012). Overall, our model of the *Sarracenia* micro-ecosystem supported the latter assertion: a focus on particular pathways (photosynthesis, decomposition) reproduced the non-linear behavior of its oxygen dynamics, including state changes and hysteresis. Additionally, the results of the sensitiv-

ity analysis suggested that the carrying capacity of the bacterial community (as it was simulated by the effect of K_w) could contribute to observed non-linear state-changes of the pitcher oxygen.

The equation representing decomposition and BOD resembles the Hill function in the general lake model. Formulating decomposition and BOD using a Hill function provided us with sufficient flexibility to yield a variety of state changes. In general, when a Hill function is used in a basic alternative states model (e.g., $rf(x) > b$ in Eq. 1), the inflection point (e.g., half-saturation constant K_w) determines the threshold (Fig. 1A). Qualitatively similar dynamics were observed in our model simulations. In the oligotrophic state, and when no prey was added, BOD remained low throughout the entire simulation (black line in (Fig. 3B). After prey was added on, for example, days 4-6 ($t = 6480$ to $t = 9360$ minutes), the system jumped into its alternative state: BOD increased rapidly then declined slowly as prey was mineralized (grey line in Fig. 3B). Although the source of the nutrients is derived from "brown", as opposed to "green" sources in lakes (*sensu* Butler et al. 2008), the similar functional shape of the pathways involved in nutrient cycling is likely to lead to similar qualitative behavior of system dynamics, suggesting that insights gained from the *Sarracenia* micro-ecosystem should be scalable to larger systems.

In the initial parameterization of this model, we started with a decomposition rate in the *Sarracenia* micro-ecosystem model in which $> 99\%$ of the average amount of prey captured could be decomposed in a single day, which was based on empirical, prey-addition studies (see Baiser et al. 2011; Sirota et al. 2013). This is extremely rapid decomposition relative to a set of 58 previously published food webs (Lau et al. 2016), in which 1.27% to 66.2% of available detritus or organic matter is decomposed each day. If the decomposition parameter (β) is 2.57E-6, the overall decomposition rate approaches the mean of the published food webs (24.22% $\pm$ 2.79 S.E.); however, this value is at the lower end of the parameter space that we used for β in our sensitivity analysis. Because photosynthesis is nutrient-limited in *Sarracenia* (Ellison 2006), addition of prey increased modeled photosynthesis (Fig. 3A) relative to oligotrophic, prey-free pitchers. The combination of the smooth, slow recovery response of photosynthesis to prey addition and the abrupt shift in BOD to prey addition (Fig. 3A & B) resulted in an abrupt shift in

the system from an oxygenated state into an anoxic state, and a very slow (hysteretic) recovery (Fig. 3C). The hysteresis of the system is clearly apparent when oxygen concentration is plotted as a time-lagged phase plot (lag = 1440 minutes starting at t=720, which shows the change in oxygen following addition of prey at t = 6480 and the slow return due to high BOD (Fig. 3D). These results agreed with observations from field and greenhouse experiments in which oxygen was observed to decline with the capture or addition of insect prey to the pitcher (Sirota et al. 2013) and demonstrated the presence of both state changes and hysteresis (i.e. Fig. 3D) for at least some parameterizations of the model.

The sensitivity analysis revealed several key effects of the BOD parameters. First, increasing w (i.e the amount of prey added) increased both the time the system was anoxic (Fig. 4A) and the return time (Fig. 4B). Second, increasing the decomposition rate (β) or K_w decreased the time that the system was anoxic, regardless of the amount of prey being added to the system (Fig. 4C). Last, and perhaps most interestingly, the effect of varying K_w on x depended on the value of β. Below $\beta < 4.0\text{E-}6$, increasing K_w increased the return time of the system, which was magnified by increasing values of w (Fig. 4D); therefore, hysteresis was observed because decreasing β slowed the recovery of the system to an oxygenated state. Similarly, for simulations with lower values of K_w, the oxygen concentration was still exponentially increasing when the simulation ended (Fig. 5A). Relative to simulations with higher K_w, the return rate was faster when β was low enough and there was prey (i.e., w_t) remaining in the pitcher at the last observed time (Fig. 5B).

The results of our model and sensitivity analyses, combined with empirical data from Sirota et al. (2013), suggest that the *Sarracenia* micro-ecosystem could be a powerful system with which to develop new understanding of the dynamics of complex ecosystems. The food web of *Sarracenia purpurea* consists of species that share an evolutionary history, organized into five trophic levels, and with interactions that have been shaped by both environmental and co-evolutionary forces (Bittleston et al. 2016; Ellison and Gotelli 2009). Both its biotic components and its abiotic environment are comparable in complexity to large lakes (Baiser et al. 2016; Kitching 2000; Srivastava et al. 2004), and it features similar critical transitions and non-linear dynamical behavior,

both of which are of broad interest for theoretical ecologists. At the same time, the dynamics of the *Sarracenia* micro-ecosystem play out over days, rather than years, decades, centuries or longer; therefore, it provides an experimental and computational model with which to identify the early warning signals of state changes in ecosystems that are of crucial importance for environmental management (Abbott and Battaglia 2015; Hoekman 2010).

References

Abbott, M. J., and L. L. Battaglia. 2015. Purple pitcher plant (Sarracenia rosea) dieback and partial community disassembly following experimental storm surge in a coastal pitcher plant bog. PLoS ONE 10.

Addicott, J. F. 1974. Predation and prey community structure: an experiment study of the effect of mosquito larvae on the protozoan communities of pitcher plants. Ecology 55:475–492.

Arber, A. 1941. On the morphology of the pitcher-leaves in \emph{Heliamphora, Sarracenia, Darlingtonia, Cephalotus}, and \emph{Nephenthes}. Annals of Botany 5:563–578.

Baiser, B., R. Ardeshiri, and A. M. Ellison. 2011. Species richness and trophic diversity increase decomposition in a co-evolved food web. PLoS One 6:e20672.

Baiser, B., R. Elhesha, and T. Kahveci. 2016. Motifs in the assembly of food web networks. Oikos 125:480–491.

Barnosky, A. D., E. A. Hadly, J. Bascompte, E. L. Berlow, J. H. Brown, M. Fortelius, W. M. Getz, J. Harte, A. Hastings, P. A. Marquet, N. D. Martinez, A. Mooers, P. Roopnarine, G. Vermeij, J. W. Williams, R. Gillespie, J. Kitzes, C. Marshall, N. Matzke, D. P. Mindell, E. Revilla, and A. B. Smith. 2012. Approaching a state shift in Earth's biosphere. Nature 486:52–8.

Bestelmeyer, B. T., A. M. Ellison, W. R. Fraser, K. B. Gorman, S. J. Holbrook, C. M. Laney, M. D. Ohman, D. P. C. Peters, F. C. Pilsbury, A. Rassweiler, R. J. Schmitt, and S. Sharma. 2011. Detecting and managing abrupt transitions in ecological systems. Ecosphere 2:129.

Biggs, R., S. R. Carpenter, and W. A. Brock. 2009. Turning back from the brink: detecting an impending regime shift in time to avert it. Proceedings of the National Academy of Sciences, USA 106:826–831.

Bittleston, L. S., N. E. Pierce, A. M. Ellison, and A. Pringle. 2016. Convergence in Multispecies Interactions. Trends in Ecology & Evolution 31:269–280.

Boynton, P. 2012. Ecological Patterns and Processes in Sarracenia Carnivorous Pitcher Plant Fungi.

Bradshaw, W. E., and R. A. Creelman. 1984. Mutualism between the carnivorous purple pitcher plant \emph{Sarracenia purpurea} and its inhabitants. American Midland Naturalist 112:294–304.

Brook, B. W., E. C. Ellis, M. P. Perring, A. W. Mackay, and L. Blomqvist. 2013. Does the terrestrial biosphere have planetary tipping points? Trends in Ecology & Evolution 28:396–401.

Butler, J. L., D. Z. Atwater, and A. M. Ellison. 2005. Red-spotted newts: an unusual nutrient source for northern pitcher plants. Northeastern Naturalist 12:1–10.

Butler, J. L., and A. M. Ellison. 2007. Nitrogen cycling dynamics in the carnivorous pitcher plant, \emph{Sarracenia purpurea}. Functional Ecology 21:835–843.

Butler, J. L., N. J. Gotelli, and A. M. Ellison. 2008. Linking the brown and green: nutrient transformation and fate in the \emph{Sarracenia} microecosystem. Ecology 89:898–904.

Carpenter, S. R. 1998. The need for large-scale experiments to assess and predict the response of ecosystems to perturbation. Pages 287–312 *in* M. L. Pace and P. M. Groffman, eds. Successes, limitations, and frontiers in ecosystem science, 12. Springer-Verlag, New York, NY.

Carpenter, S. R., and W. A. Brock. 2006. Rising variance: a leading indicator of ecological transition. Ecology Letters 9:311–318.

Carpenter, S. R., D. L. Christensen, J. J. Cole, K. L. Cottingham, X. He, J. R. Hodgson, J. F. Kitchell, S. E. Knight, M. L. Pace, and . et al. 1995. Biological Control of Eutrophication in Lakes. Environmental Science & Technology 29:784–786.

Carpenter, S. R., J. J. Cole, M. L. Pace, R. Batt, W. A. Brock, T. Cline, J. Coloso, J. R. Hodgson, J. F. Kitchell, D. A. Seekell, L. Smith, and B. Weidel. 2011. Early warnings of regime shifts: a whole-ecosystem experiment. Science 332:1079–1082.

Chislock, M. F., E. Doster, R. A. Zitomer, and A. E. Wilson. 2013. Eutrophication: Causes, Consequences, and Controls in Aquatic Ecosystems. Nature Education Knowledge 4:10.

Cochran-Stafira, D. L., and C. N. von Ende. 1998. Integrating bacteria into food webs: studies with Sarracenia purpurea inquilines. Ecology 79:880–898.

Contamin, R., and A. M. Ellison. 2009. Indicators of regime shifts in ecological systems: what do we need to know and when do we need to know it? Ecological Applications 19:799–816.

Dakos, V., S. R. Carpenter, W. A. Brock, A. M. Ellison, V. Guttal, A. R. Ives, S. Kéfi, V. Livina, D. A. Seekell, E. H. van Nes, and M. Scheffer. 2012. Methods for detecting early warnings of critical transitions in time series illustrated using simulated ecological data. PloS one 7:e41010.

Ellison, A. M. 2006. Nutrient limitation and stoichiometry of carnivorous plants. Plant Biologyogy 8:740–747.

Ellison, A. M., and N. J. Gotelli. 2009. Energetics and the evolution of carnivorous plants - Darwin's "most wonderful plants in the world". Journal of Experimental Botany 60:19–42.

Gallie, D. R., and S. C. Chang. 1997. Signal transduction in the carnivorous plant \emph{Sarracenia purpurea} - Regulation of secretory hydrolase expression during development and in response to resources. Plant Physiology 115:1461–1471.

Givnish, T. J., E. L. Burkhardt, R. E. Happel, and J. D. Weintraub. 1984. Carnivory in the bromeliad \emph{Brocchinia reducta}, with a cost/ benefit model for the general restriction of carnivorous plants to sunny, moist nutrient-poor habitats. American Naturalist 124:479–497.

Heard, S. B. 1994. Pitcher plant midges and mosquitoes: a processing chain commensalism. Ecology 75:1647–1660.

Hoekman, D. 2010. Turning up the heat: Temperature influences the relative importance of top-down and bottom-up effects. Ecology 91:2819–2825.

Jones, F. M. 1923. The most wonderful plant in the world. Natural History 23:589–596.

Kingsolver, J. G. 1979. Thermal and Hydric Aspects of Environmental Heterogeneity in the Pitcher Plant Mosquito. Ecological Monographs 49:357–376.

Kitching, R. L. 2000. Food webs and container habitats : the natural history and ecology of phytotelmata. Cambridge University Press Cambridge.

Lau, M. K., S. R. Borrett, D. E. Hines, and P. Singh. 2016. enaR: Tools for Ecological Network Analysis.

Levine, N. M., K. Zhang, M. Longo, A. Baccini, O. L. Phillips, S. L. Lewis, E. Alvarez-Dávila, A. C. Segalin de Andrade, R. J. W. Brienen, T. L. Erwin, T. R. Feldpausch, A. L. Monteagudo Mendoza, P. Nuñez Vargas, A. Prieto, J. E. Silva-Espejo, Y. Malhi, and P. R. Moorcroft. 2016. Ecosystem heterogeneity determines the ecological resilience of the Amazon to climate change. Proceedings of the National Academy of Sciences 113:793–797.

McCann, K. S. 2012. Food Webs (MPB-50). Princeton University Press.

Mittlebach, G. G., A. M. Turner, D. J. Hall, J. E. Rettig, and C. W. Osenberg. 1995. Perturbation and resilience: a long-term, whole-lake study of predator extinction and reintroduction. Ecology 76:2347–2360.

Mulder, C., and A. J. Hendriks. 2014. Half-saturation constants in functional responses. Global Ecology and Conservation 2:161–169.

Peterson, C. N., S. Day, B. E. Wolfe, A. M. Ellison, A. M. Kolter, and A. Pringle. 2008. A keystone predator controls bacterial diversity in the pitcher plant (Sarracenia purpurea) microecosystem. Environmental Microbiology 10:2257–2266.

Petraitis, P. S., and S. R. Dudgeon. 2016. Cusps and butterflies: multiple stable states in marine systems as catastrophes. Marine and Freshwater Research 67:37.

R Core Team. 2016. R: A Language and Environment for Statistical Computing.

Scheffer, M., J. Bascompte, W. A. Brock, V. Brovkin, S. R. Carpenter, V. Dakos, H. Held, E. H. van Nes, M. Rietkerk, and G. Sugihara. 2009. Early-warning signals for critical transitions. Nature 461:53–59.

Scheffer, M., S. Carpenter, J. A. Foley, C. Folke, and B. Walker. 2001. Catastrophic shifts in ecosystems. Nature 413:591–596.

Schnell, D. E. 2002. Carnivorous plants of the United States and Canada, vol. 2. Timber Press, Portland, Oregon, USA.

Sirota, J., B. Baiser, N. J. Gotelli, and A. M. Ellison. 2013. Organic-matter loading determines regime shifts and alternative states in an aquatic ecosystem. Proceedings of the National Academy of Sciences 110:7742–7747.

Srivastava, D. S., J. Kolasa, J. Bengtsson, A. Gonzalez, S. P. Lawler, T. E. Miller, P. Munguia, T. Romanuk, D. C. Schneider, and M. K. Trzcinski. 2004. Are natural microcosms useful model systems for ecology? Trends Ecol.Evol 19:379–384.

Ulanowicz, R. E. 2012. Growth and Development: Ecosystems Phenomenology. Springer Science & Business Media.

Wood, K. A., M. T. O'Hare, C. McDonald, K. R. Searle, F. Daunt, and R. A. Stillman. 2016. Herbivore regulation of plant abundance in aquatic ecosystems. Biological Reviews .

Table 1: Terms, units, and interpretation for the model of oxygen dynamics in pitcher plant fluid.

Term	Units	Interpretation
t	minutes	time (model iteration)
f	$1/t$	Constant adjusting sine wave of diurnal PAR for frequency of measurements
x_t	mg/L	$[O_2]$: concentration of oxygen in the pitcher fluid
Photosynthesis		
A_t	mg/L	Production of oxygen by photosynthesis and infused from the plant into the fluid during the day
a_t	mg/L	Photosynthetic rate augmentation by microbial nutrient mineralization
a_{min}, a_{max}	mg/L	Min or max possible photosynthetic augmentation
PAR	$\mu\text{mol} \cdot \text{m}^{-2} \cdot \text{s}^{-1}$	Photosynthetically active radiation
Respiration		
w_t	mg	Mass of prey remaining at time t
W	mg	Maximum mass of decomposable prey (set at 75μ g)
K_w	mg/min	Half-saturation constant for bacterial carrying capacity
m	mg/L	Basal metabolic oxygen used by bacteria (respiration)
Nutrients		
n_t	mg/L	Quantity of nutrients mineralized by decomposition; a function of w_t and x_t
s	dimensionless	Sigmoidal curve steepness relating nutrient mineralization to augmentation
d	mg	Inflection point of sigmoidal curve relating mineralization to augmentation
β	dimensionless	The rate of prey decomposition

Figure legends

Figure 1: The threshold dynamics of the Hill function are determined in part by the inflection parameter h. A) Plotted output of the Hill function for different values of h (different lines shaded darker for lower values), which range from 0.1 to 150 with $p = 10$. B) Lagged ($k = 1$ lag term) phase-plot of the Hill function with $h = 71.11$, showing the state transition (lower-left to upper-right). A small amount of random variation was introduced to the series to reveal overlapping points within the two states.

Figure 2: A) The pitcher plant model shown as a network diagram. The nodes in the graph and their corresponding variables in the model are *Prey* (w), the microbially dominated *Food Web* (controlled by K_w), Nitrogen (n), Oxygen (x) and the *Pitcher Plant*, which is included to show the fluxes of nitrogen and oxygen as they relate to the plant itself. B) The sine wave of Photosynthetically Active Radiation (PAR) from the sun or other light source. C) The relationship between PAR and photosynthesis in the pitcher plant. D) The output of dissolved oxygen in the pitcher fluid as a function of pitcher plant photosynthesis. E) The decomposition of prey over time as effected by the food-web, primarily bacteria. F) The impact of prey addition (t = 2160) on pitcher plant photosynthesis.

Figure 3: The addition of prey impacts both photosynthetic oxygen production via augmentation by mineralization and oxygen depletion through the biological oxygen demand (BOD) of microbial metabolism. The scatterplot (A) shows how photosynthesis increased when prey was added (grey) on days 4-6 (t = 5040 to t = 7920 minutes), relative to when no prey was added (black). (B) shows the quantity of oxygen used via the BOD of microbial decomposition. The net impact in this parameterization was a net decrease in dissolved oxygen when prey was added to the system, as seen in plot (C), which shows the dynamic of oxygen present in the pitcher at mid-day. (D) A time lagged phase plot (with a lag 1440 min. starting at $t = 720$) showing the change in oxygen production in the prey addition simulation induced by the addition and subsequent decomposition of prey entering the system at $t = 5040$ and the altered return trajectory (i.e., hysteresis) resulting from the associated oxygen demand of the food web decomposing in the system shown by the arrows indicating the direction of the change in oxygen through time.

Figure 4: Sensitivity analysis for the pitcher plant model showing the non-linear effect of the parameters w, β and K_w (n = 15000). The plots of the spline $\pm$ 1 S.D. in (A) and (B) show that w increases the Percent Time Anoxic and the Return Rate, respectively, regardless of the the value of β and K_w. Changes in β and K_w had non-linear impacts on the resulting anoxia of the system (C). However, changes in β and K_w had interactive effects on the Return Rate with values of β below a threshold ($\leq$ 4.0E-6) leading to non-linearly increasing Return Rates with larger values of K_w and values of β above that threshold leading to decreasing Return Rates with increasing K_w with the shape of the decrease ranging from nearly linear to non-linear depending on the amount of prey added to the system (i.e., w).

Figure 5: The dynamics of pitcher plant oxygen for three simulations at different levels of K_w (black = 0.1, dark-grey = 0.5 and light-grey = 1) with the same rate of decomposition (β = 2.0E-6) illustrating the hysteresis (i.e., altered return trajectory) of the system. (A) Lower levels of K_w produce slower return rates over the course of the simulation, evidenced by depressed mid-day oxygen curves at lower values of K_w. (B) A time lagged (t = 1440) phase plot for the same simulations showing that lower values of K_w lead to the oxygen dynamics of the system spending more time at lower levels of oxygen, but follow a similar trajectory as prey is removed from the system by the food-web.

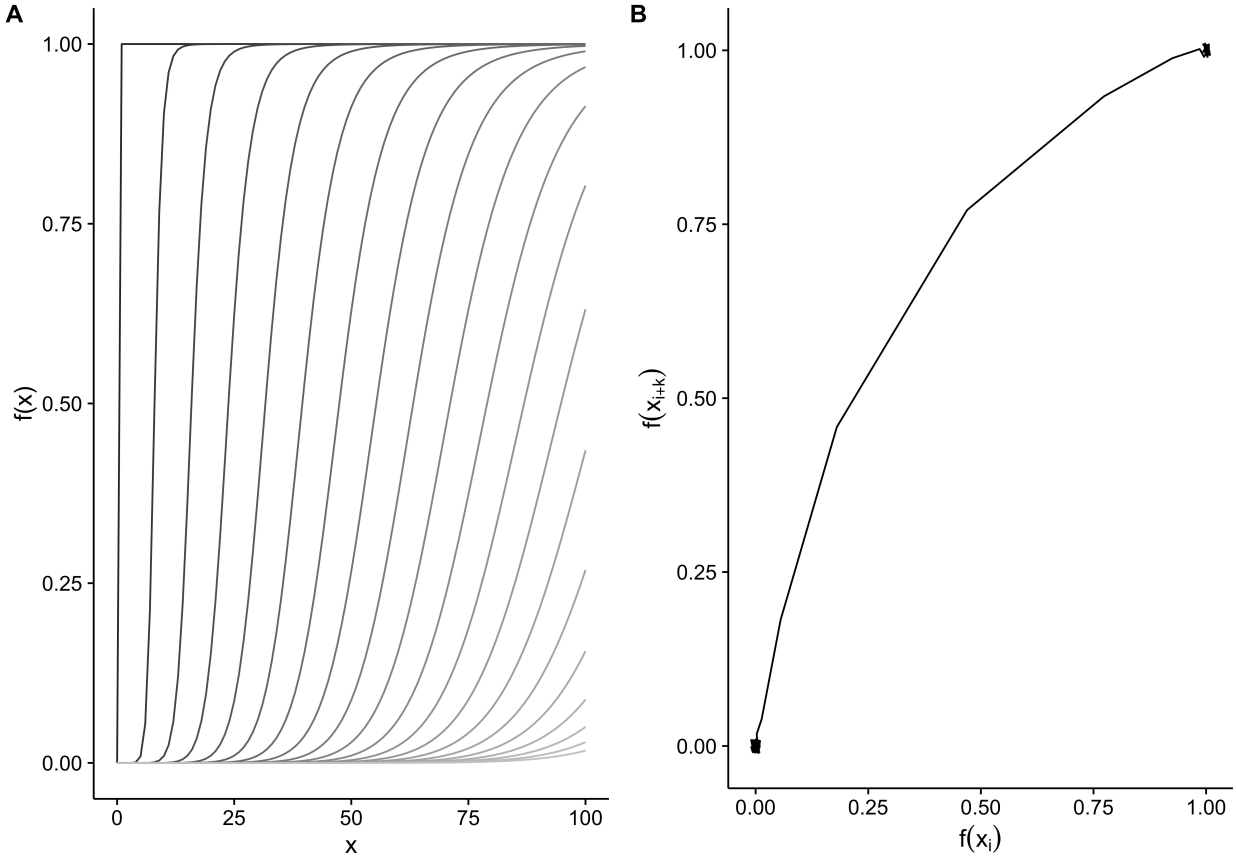
A
1.00
0.75
0.50
0.25
0.00
f(x)
0
25
50
75
100
x
B
1.00
0.75
0.50
0.25
0.00
f(x_{i+k})
0.00
0.25
0.50
0.75
1.00
f(x_i)

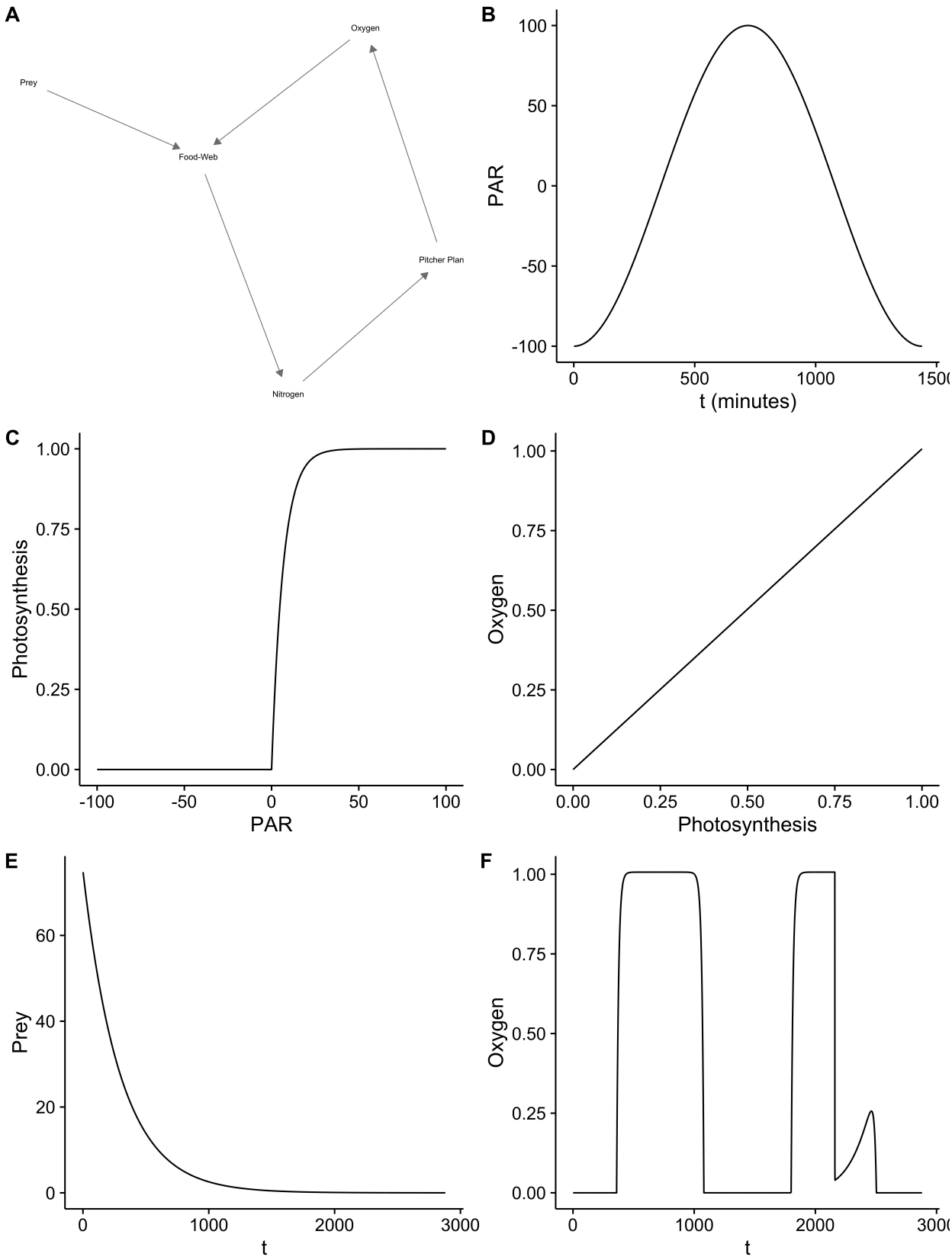
A
Oxygen
Prey
Food-Web
Pitcher Plan
Nitrogen
B
PAR
t (minutes)
C
Photosynthesis
PAR
D
Oxygen
Photosynthesis
E
Prey
t
F
Oxygen
t

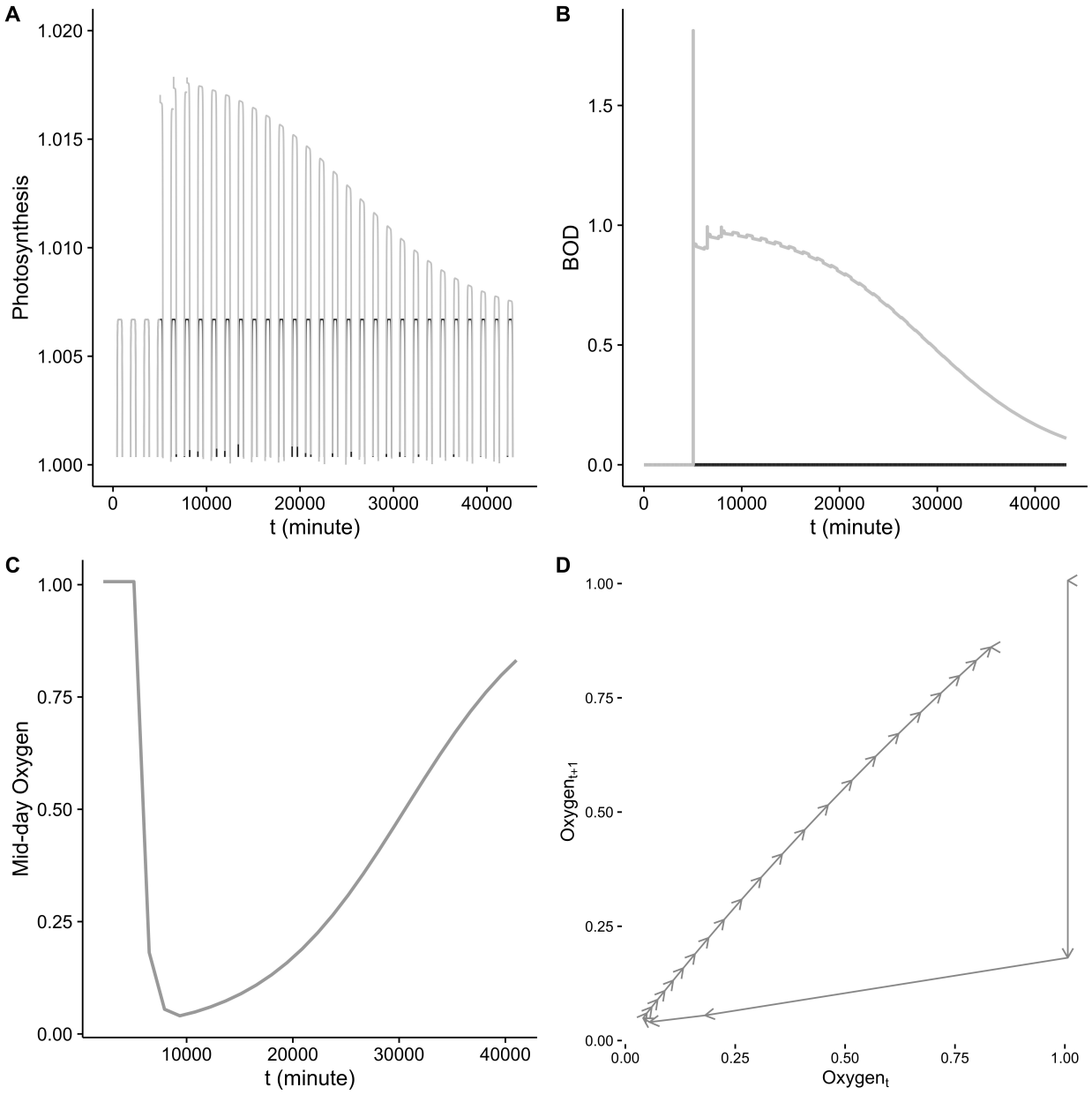
A
Photosynthesis
1.020
1.015
1.010
1.005
1.000
0
10000
20000
30000
40000
t (minute)
B
BOD
1.5
1.0
0.5
0.0
0
10000
20000
30000
40000
t (minute)
C
Mid-day Oxygen
1.00
0.75
0.50
0.25
0.00
10000
20000
30000
40000
t (minute)
D
Oxygen$_{t+1}$
1.00
0.75
0.50
0.25
0.00
0.00
0.25
0.50
0.75
1.00
Oxygen$_t$

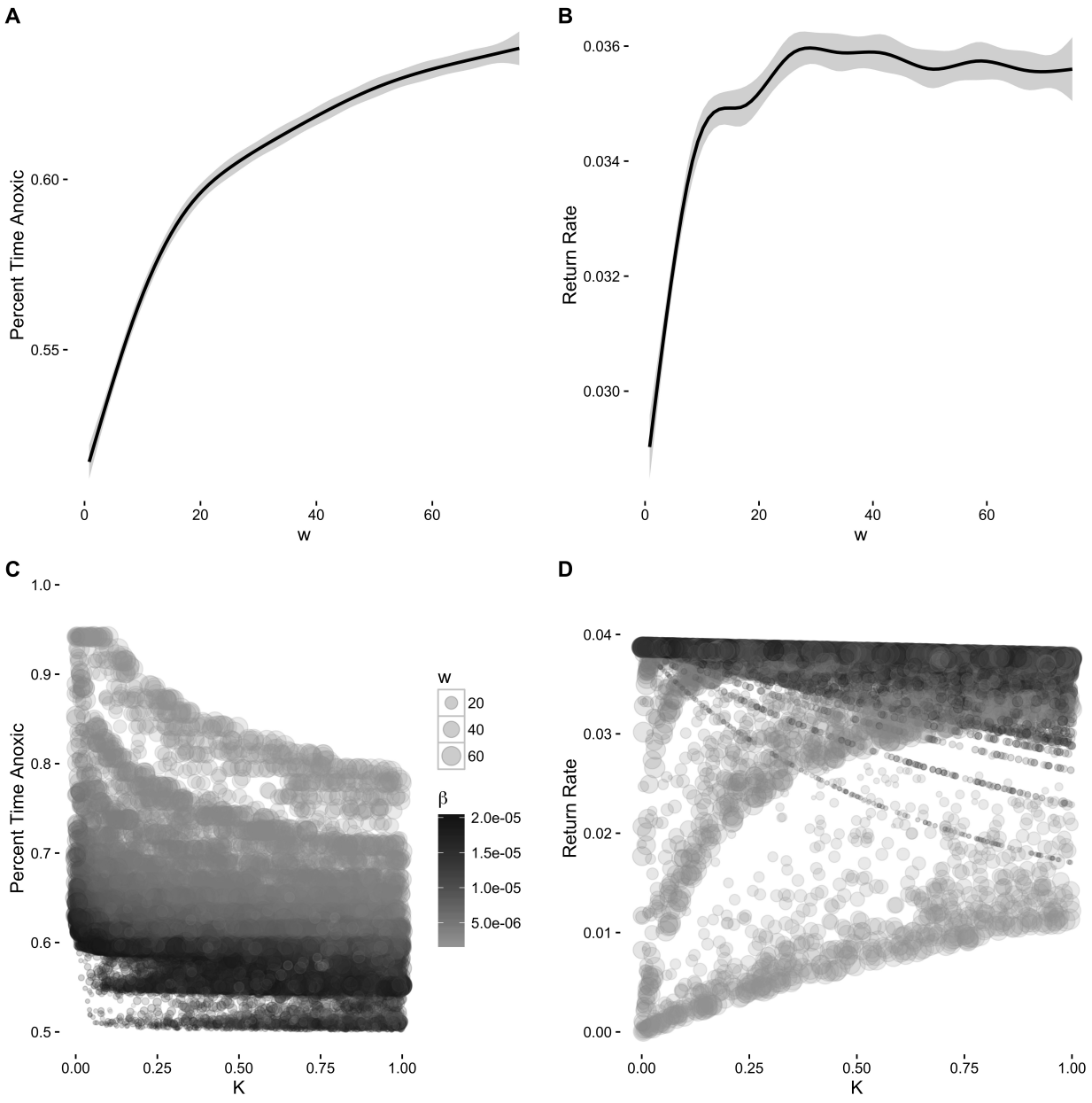
A
Percent Time Anoxic
0.60
0.55
0
20
40
60
w
B
Return Rate
0.036
0.034
0.032
0.030
0
20
40
60
w
C
Percent Time Anoxic
1.0
0.9
0.8
0.7
0.6
0.5
0.00
0.25
0.50
0.75
1.00
K
w
20
40
60
β
2.0e-05
1.5e-05
1.0e-05
5.0e-06
D
Return Rate
0.04
0.03
0.02
0.01
0.00
0.00
0.25
0.50
0.75
1.00
K

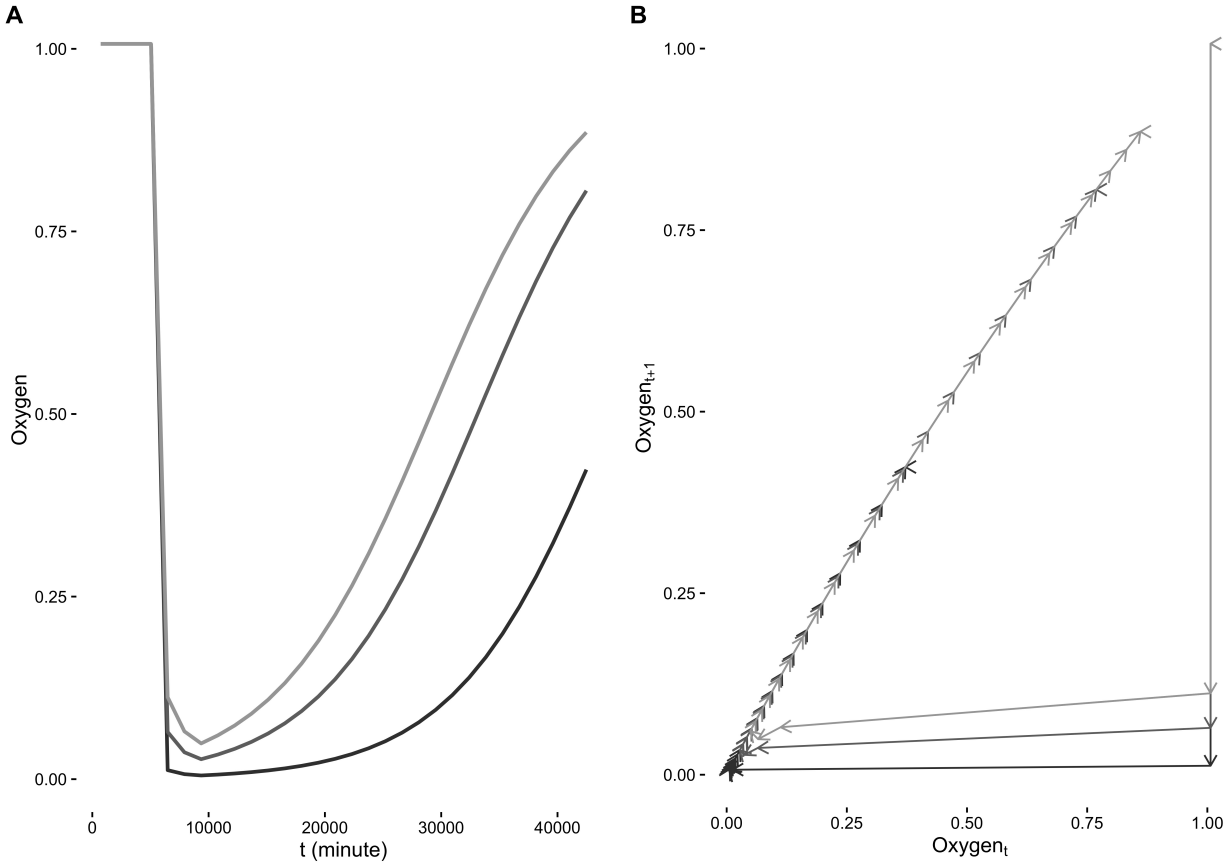
A
1.00
0.75
0.50
0.25
0.00
Oxygen
0
10000
20000
30000
40000
t (minute)
B
1.00
0.75
0.50
0.25
0.00
Oxygen$_{t+1}$
0.00
0.25
0.50
0.75
1.00
Oxygen$_t$